Magnetic particle hyperthermia: Néel relaxation in magnetic nanoparticles under circularly polarized field

2009 J. Phys.: Condens. Matter 21 124202

(http://iopscience.iop.org/0953-8984/21/12/124202)

J. Phys.: Condens. Matter **21** (2009) 124202 (8pp) doi:10.1088/0953-8984/21/12/124202

Magnetic particle hyperthermia: Néel relaxation in magnetic nanoparticles under circularly polarized field

P F de Châtel[1,2], I Nándori[1], J Hakl[1], S Mészáros[1] and K Vad[1]

[1] Institute of Nuclear Research, PO Box 51, H-4001 Debrecen, Hungary
[2] Institute of Metal Research, Chinese Academy of Sciences, Shenyang 110016, People's Republic of China

Received 27 September 2008, in final form 2 December 2008
Published 25 February 2009
Online at stacks.iop.org/JPhysCM/21/124202

Abstract
The mechanism of magnetization reversal in single-domain ferromagnetic particles is of interest in many applications, in most of which losses must be minimized. In cancer therapy by hyperthermia the opposite requirement prevails: the specific loss power should be maximized. Of the mechanisms of dissipation, here we study the effect of Néel relaxation on magnetic nanoparticles unable to move or rotate and compare the losses in linearly and circularly polarized fields. We present exact analytical solutions of the Landau–Lifshitz equation as derived from the Gilbert equation and use the calculated time-dependent magnetizations to find the energy loss per cycle. In frequencies lower than the Larmor frequency, linear polarization is found to be the better source of heat power, at high frequencies (beyond the Larmor frequency) circular polarization is preferable.

1. Introduction

The dynamics of the magnetization of single-domain ferromagnetic bodies under various conditions has been studied with widely different motivations. Ferromagnetic resonance has provided perhaps the best known example. In this case a strong static magnetic field **B** generates and stabilizes the single-domain state. The torque $\mathbf{G} = \boldsymbol{\mu} \times \mathbf{B}$ exercised by this field, being perpendicular to **B**, causes a precession of the magnetic moment $\boldsymbol{\mu}$ around the field, leaving the angle between $\boldsymbol{\mu}$ and **B** intact. The resonance is detected by means of an alternating field perpendicular to **B**, whose energy is absorbed at a maximum rate at the Larmor frequency, $\omega_{\mathrm{L}} = \gamma|\mathbf{B}|$.

Without a strong static field, in a sizable sample the single-domain state can only be achieved in a material of extremely large permeability. This requirement dictated the choice of 'soft iron' in the famous Einstein–de Haas experiment [1], which provided the first experimental determination of the gyromagnetic ratio γ. The limitation to soft magnetic materials can be circumvented though with very small samples. Clearly, samples smaller than the domain–wall thickness cannot contain more than one domain.

The dynamics of the magnetic moment of nanometre-sized single-domain particles is of interest in connection with a number of applications. In magnetic recording, the processes taking place in magnetized particles under minor perturbations (reading) and during magnetization reversal (switching) are of paramount interest. In this case, the nanoparticles are immobile, their place and orientation are fixed. A fast process of magnetization reversal with minimal losses is the most important requirement for applicability in magnetic recording.

Ferrofluids contain mobile magnetic nanoparticles, whose position and orientation can be controlled by a magnetic field. In their application in hyperthermia, the most important requirement is the absorption of large losses under repeated magnetization reversal. More precisely, the figure of merit to be maximized is the specific absorption rate (also called the specific loss rate or heating rate), i.e. the amount of energy absorbed per second by a unit mass of magnetic nanoparticles. The conditions under which maximization has to be realized are quite demanding, as they are dictated by biophysical factors [2].

The mobility of magnetic particles in ferrofluids is an important feature in the context of losses under repeated magnetization reversal. As the particles are free to rotate, the potential energy $E = -\boldsymbol{\mu} \cdot \mathbf{B}$ can be minimized in two ways: either the magnetic moment rotates within the particle until it is aligned with the field, or the particle rotates as a whole. Two

different processes are involved, Néel and Brown relaxation, respectively. In the latter the energy is transferred directly to the fluid, due to the viscous flow arising at the surface of the particle. In Néel relaxation the energy is transferred to the lattice, i.e. it is absorbed by phonons and magnons, before ordinary heat transport conveys it to the fluid. Both processes are characterized by appropriate relaxation times, τ_N and τ_B, a parameterization that conceals the difference between the two mechanisms. The apparent similarity is further emphasized by the term 'magnetic viscosity', a misleading synonym for Néel relaxation.

The common practice in hyperthermia is to expose magnetic nanoparticles present in a ferrofluid, preferably inside the malignant tumours, to a magnetic field alternating at a frequency of the order of 10^5 Hz. The optimization of loss energy with respect to the amplitude and frequency of this linearly polarized field has been studied in detail [3]. However, the effect of circularly polarized field received relatively little attention. This neglect is not justified though, as there is no obvious reason why the specific absorption rate should be indifferent to the nature of polarization.

In the present paper we report on the first stage of a systematic theoretical study of the dynamic response of a system of magnetic nanoparticles to linearly and circularly polarized magnetic field. The ultimate goal of this study is an analysis of the criteria for a maximum output of heating power applicable in hyperthermia. The relative importance of Néel and Brown relaxations is not clear. Hergst *et al* [2] have made susceptibility measurements on a colloidal suspension of maghemite (γFe_2O_3) particles at frequencies ranging from 10 Hz and 1 MHz. The very broad peak in the imaginary part of the susceptibility found at 1 kHz disappeared when the particles were made immobile by letting the solvent freeze. In this case, viscous losses (Brownian relaxation) are clearly dominant. On the other hand, these authors also pointed out that the mobility of particles trapped in tumour tissue is not known. If they are clogged to the extent of not being able to rotate, the Néel mechanism is the only relaxation process available. Here we present analytical results for an immobilized single-domain particle. In section 2 we briefly summarize the theoretical tools available for the study of the Néel mechanism and recapitulate the relation between the Landau–Lifshitz and Gilbert equations. Section 3 treats the case of linearly polarized magnetic fields, for which we present exact analytical solutions of the Landau–Lifshitz equation, which are used to determine the heating power as a function of frequency and amplitude of the alternating field. In section 4 approximate analytic solutions are presented for circular polarization, which are exact under specific initial conditions. For arbitrary initial conditions, those solutions give an exact description of the dynamics in the steady state, which is stabilized after a short initial transient time-interval. The heating power is calculated for this steady state.

2. Néel relaxation

We shall describe the magnetization processes in an isotropic single-domain particle by means of the Landau–Lifshitz equation [4], which is generally used to consider the Néel relaxation mechanism [5] of magnetic nanoparticle systems. It is customary to write the Landau–Lifshitz equation in the form

$$\frac{\mathrm{d}}{\mathrm{d}t}\mathbf{m} = \mu_0\gamma\left([\mathbf{m}\times\mathbf{H}] + \frac{\alpha}{m_S}[[\mathbf{m}\times\mathbf{H}]\times\mathbf{m}]\right), \qquad (1)$$

where $\mathbf{m} = \boldsymbol{\mu}/V$, V is the volume of the particle, $\mu_0 = 4\pi \times 10^{-7}$ N A^{-2} is the permeability of free space, γ is an effective gyromagnetic ratio, α is a dimensionless damping constant, m_S is the saturation magnetization and $\mathbf{H} = \mu_0^{-1}\mathbf{B}$ is the applied magnetic field. Formally, the Gilbert equation [6],

$$\frac{\mathrm{d}}{\mathrm{d}t}\mathbf{m} = \mu_0\gamma_0\left([\mathbf{m}\times\mathbf{H}] - \eta\left[\mathbf{m}\times\frac{\mathrm{d}}{\mathrm{d}t}\mathbf{m}\right]\right) \qquad (2)$$

is equivalent to the Landau–Lifshitz equation, as can be verified [6] with the identifications $\alpha = \mu_0\gamma_0\eta m_S$ and $\gamma = \gamma_0/(1+\alpha^2)$ of the parameters of the latter in terms of those of the former. Here $\gamma_0 = 8.82 \times 10^{10}$ Am^2 J^{-1} s^{-1} is the gyromagnetic ratio of the electron and η is the damping constant. As pointed out by Kikuchi [8], the factor $1/(1+\alpha^2)$ appearing on the right-hand side of the Landau–Lifshitz equation as derived from the Gilbert equation removes a 'physically implausible situation' [9] in the predicted behaviour at large damping.

The most conspicuous feature of the Landau–Lifshitz equation is that the vector standing on the right-hand side is perpendicular to the magnetization vector. It follows then that $\mathrm{d}m^2/\mathrm{d}t = \mathbf{m}\cdot\mathrm{d}\mathbf{m}/\mathrm{d}t = 0$, that is, the magnetization vector's magnitude does not change under the influence of the external field. Therefore, it is convenient to rewrite equation (1) in terms of the unit vector $\mathbf{M} = \mathbf{m}/m_S$:

$$\frac{\mathrm{d}}{\mathrm{d}t}\mathbf{M} = \gamma'[\mathbf{M}\times\mathbf{H}] - \alpha'[[\mathbf{M}\times\mathbf{H}]\times\mathbf{M}]. \qquad (3)$$

The new coefficients are given in terms of the ones in equations (1) and (2) as $\gamma' = \mu_0\gamma = \mu_0\gamma_0/(1+\alpha^2)$ and $\alpha' = \mu_0\gamma\alpha = \mu_0^2\gamma_0^2\eta m_S/(1+\alpha^2)$. With these definitions of the coefficients, equation (3) is the Landau–Lifshitz equation as derived from the Gilbert equation [7], which will be referred to as the Landau–Lifshitz–Gilbert (LLG) equation in what follows.

3. Linearly polarized applied field

In this section, we present an exact analytic solution for the LLG equation (3) for an isotropic magnetic particle subjected to a linearly polarized, i.e. alternating, applied magnetic field. The results enable the numerical evaluation of the heating rate per particle. The alternating field is assumed to be applied in the x direction,

$$\mathbf{H} = \frac{\omega_L}{\gamma'}(\cos(\omega t), 0, 0), \qquad (4)$$

where $\omega_L = \gamma'|\mathbf{H}|$ is the Larmor frequency, ω is the angular frequency of the alternating external magnetic field.

3.1. Free precession

In the case of vanishing relaxation ($\alpha' = 0$), the LLG equations for the Cartesian components of the magnetization vector are

$$\begin{aligned} \frac{\mathrm{d}}{\mathrm{d}t}M_x &= 0, \\ \frac{\mathrm{d}}{\mathrm{d}t}M_y &= \cos(\omega t)\,\omega_\mathrm{L} M_z, \\ \frac{\mathrm{d}}{\mathrm{d}t}M_z &= -\cos(\omega t)\,\omega_\mathrm{L} M_y. \end{aligned} \tag{5}$$

The analytical solution of these coupled equations for all possible initial conditions can be written as

$$\begin{aligned} M_x(t) &= M_{x0}, \\ M_y(t) &= \sqrt{1-M_{x0}^2}\ \sin\left[\frac{\omega_\mathrm{L}}{\omega}\sin(\omega t)+\delta_0\right], \\ M_z(t) &= \sqrt{1-M_{x0}^2}\ \cos\left[\frac{\omega_\mathrm{L}}{\omega}\sin(\omega t)+\delta_0\right], \end{aligned} \tag{6}$$

where M_{x0} and δ_0 are determined by the initial conditions: $M_{x0} = M_x(0)$ and $\delta_0 = \tan^{-1}(M_y(0)/M_z(0))$. The interpretation of equation (6) is that the unit vector representing the magnetization is precessing around the x axis with a time-dependent angular velocity. At time t, its projection on the yz plane is at an angle $\delta(t) = \tan^{-1}(M_y(t)/M_z(t)) = [(\omega_\mathrm{L}/\omega)\sin(\omega t) + \delta_0]$ from the z axis. The angular velocity of the precession is changing periodically. If $(\omega_\mathrm{L}/\omega) \gg 1$, precession in a given sense prevails for many full cycles, before it slows down and changes sign. For the static limit, i.e. $\omega \to 0$, the solution (6) reduces to

$$\begin{aligned} M_x(t) &= M_{x0}, \\ M_y(t) &= \sqrt{1-M_{x0}^2}\,\sin[\omega_\mathrm{L} t+\delta_0], \\ M_z(t) &= \sqrt{1-M_{x0}^2}\,\cos[\omega_\mathrm{L} t+\delta_0]. \end{aligned} \tag{7}$$

This is the limit when the period of the alternating field is so long that the Larmor precession seems to proceed uninterrupted. In the opposite limit, $(\omega_\mathrm{L}/\omega) \ll 1$, there is only an oscillation of small amplitude about δ_0 (i.e. $\delta(t) \approx \delta_0$).

3.2. Damped precession

In the presence of Néel relaxation, the LLG equations for the Cartesian components of the magnetization for linearly polarized applied field are

$$\begin{aligned} \frac{\mathrm{d}}{\mathrm{d}t}M_x &= \alpha_\mathrm{N}\cos(\omega t)(1-M_x^2), \\ \frac{\mathrm{d}}{\mathrm{d}t}M_y &= \cos(\omega t)(\omega_\mathrm{L} M_z - \alpha_\mathrm{N} M_x M_y), \\ \frac{\mathrm{d}}{\mathrm{d}t}M_z &= -\cos(\omega t)(\omega_\mathrm{L} M_y + \alpha_\mathrm{N} M_x M_z), \end{aligned} \tag{8}$$

where we have introduced $\alpha_\mathrm{N} = \alpha'|\mathbf{H}|$ as a measure of damping. The analytical solution is

$$\begin{aligned} M_x(t) &= \frac{(M_{x0}-1)+(M_{x0}+1)\exp\left[\frac{2\alpha_\mathrm{N}}{\omega}\sin(\omega t)\right]}{(1-M_{x0})+(M_{x0}+1)\exp\left[\frac{2\alpha_\mathrm{N}}{\omega}\sin(\omega t)\right]} \\ &= \frac{\tanh\left(\frac{\alpha_\mathrm{N}}{\omega}\sin(\omega t)\right)+M_{x0}}{1+M_{x0}\tanh\left(\frac{\alpha_\mathrm{N}}{\omega}\sin(\omega t)\right)}, \\ M_y(t) &= \sqrt{1-M_x^2(t)}\ \sin\left[\frac{\omega_\mathrm{L}}{\omega}\sin(\omega t)+\delta_0\right], \\ M_z(t) &= \sqrt{1-M_x^2(t)}\ \cos\left[\frac{\omega_\mathrm{L}}{\omega}\sin(\omega t)+\delta_0\right], \end{aligned} \tag{9}$$

where, as before, M_{x0} and δ_0 are determined by the initial conditions: $M_{x0} = M_x(0)$ and $\delta_0 = \tan^{-1}(M_y(0)/M_z(0))$. The interpretation of equation (9) is that, as in the absence of relaxation, the unit vector representing the magnetization is precessing around the x axis with a time-dependent angular velocity, but in this case the angle β between the **M** vector and the x axis changes as $\beta = \cos^{-1}(M_x(t))$. At time t, the projection of **M** on the yz plane has a length of $\sin(\beta)$ and is at an angle $\delta(t) = \tan^{-1}(M_y(t)/M_z(t)) = [(\omega_\mathrm{L}/\omega)\sin(\omega t)+\delta_0]$ from the z axis. The angular velocity of the precession and the projected length of the unit vector **M** are changing periodically. If $(\alpha_\mathrm{N}/\omega) \ll 1$ and $(\omega_\mathrm{L}/\omega) \gg 1$ the precessing unit vector approaches the x axis slowly, completing many cycles before it slows down and changes sign. Note that the first condition can be fulfilled both at very weak and very strong damping, since $\alpha_\mathrm{N} \propto (1+\alpha^2)^{-1}$. For $(\alpha_\mathrm{N}/\omega) \gg 1$ the precessing unit vector quickly approaches the direction of the driving field, it is very close to being aligned with the x axis, alternating between the positive and negative directions. For vanishingly weak or infinitely strong damping, that is in the $\alpha_\mathrm{N} \to 0$ limit, the solution reduces to equation (6). For the static limit, i.e. $\omega \to 0$ the general solution (9) reduces to

$$\begin{aligned} M_x(t) &= \frac{(M_{x0}-1)+(M_{x0}+1)\exp[2\alpha_\mathrm{N} t]}{(1-M_{x0})+(M_{x0}+1)\exp[2\alpha_\mathrm{N} t]} \\ &= \frac{\tanh(\alpha_\mathrm{N} t)+M_{x0}}{1+M_{x0}\tanh(\alpha_\mathrm{N} t)}, \\ M_y(t) &= \sqrt{1-M_x^2(t)}\,\sin[\omega_\mathrm{L} t+\delta_0], \\ M_z(t) &= \sqrt{1-M_x^2(t)}\,\cos[\omega_\mathrm{L} t+\delta_0]. \end{aligned} \tag{10}$$

In this case the **M** vector is precessing with a time-independent angular velocity ω_L and converges towards the $+x$ direction with a time constant $\sim 1/\alpha_\mathrm{N}$. In practice, for $H \approx 10^4$ A m^{-1}, we find that $\alpha_\mathrm{N} = \mu_0\gamma_0 H\alpha/(1+\alpha^2) \approx \alpha/(1+\alpha^2)\times 10^9$ s^{-1}, so that even for weak damping, e.g. $\alpha = 0.001$, the convergence is very fast, M_y and M_z vanish within a few microseconds. This implies that for frequencies much lower than 1 MHz we have $M_x(t) \cong 1$.

3.3. Specific loss power

The results given above enable us to calculate the energy loss for a single particle. The energy dissipated in a single cycle

can be calculated as

$$E = \mu_0 \int_0^{2\pi/\omega} \mathrm{d}t \left(\mathbf{H} \cdot \frac{\mathrm{d}\mathbf{m}}{\mathrm{d}t} \right) = \mu_0 m_\mathrm{S} \int_0^{2\pi/\omega} \mathrm{d}t \left(\mathbf{H} \cdot \frac{\mathrm{d}\mathbf{M}}{\mathrm{d}t} \right). \tag{11}$$

Using the expression (4) for **H** and the LLG equation (8) and its solution equation (9), the energy dissipated in a single cycle,

$$E = \mu_0 m_\mathrm{S} \alpha_\mathrm{N} H \int_0^{2\pi/\omega} \mathrm{d}t \, [\cos(\omega t)]^2 \, [1 - M_x^2(t)], \tag{12}$$

can be calculated numerically. The loss per cycle depends on the initial conditions, it has a maximum when $M_{x0} = 0$.

Analytical results are available in the limit of $(\alpha_\mathrm{N}/\omega) \ll 1$ where $M_x(t)$ can be expanded in powers of α_N/ω. As in the initial state, in a ferrofluid the magnetization vectors are randomly distributed, the relevant quantity will be the average of the loss power (12) over this distribution. To lowest order in α_N/ω this gives

$$E_\mathrm{average} \approx \frac{2}{3} \mu_0 \pi m_\mathrm{S} H \frac{\alpha_\mathrm{N}}{\omega}. \tag{13}$$

At frequencies much lower than 1 MHz ($\alpha_\mathrm{N}/\omega \gg 1$), the loss per cycle becomes independent of the initial conditions and frequency. In this limit

$$E_\mathrm{average} \approx E = 4\mu_0 m_\mathrm{S} H. \tag{14}$$

4. Circularly polarized applied field

Here, we present analytical solutions of the LLG equations for an immobile single-domain magnetic particle under circularly polarized, i.e. rotating, applied magnetic field. Our exact analytical solutions are only valid for specific initial conditions. However, they also give the correct answer if one is interested in the behaviour in the steady state that sets in after a short relaxation process. The heating loss per cycle of a single particle in this state will be calculated to be compared in the next section to that obtained for the linearly polarized field.

The applied field is assumed to rotate in the xy plane with an angular frequency ω

$$\mathbf{H} = \frac{\omega_\mathrm{L}}{\gamma'} (\cos(\omega t), \sin(\omega t), 0). \tag{15}$$

We also introduce the angular velocity vector $\boldsymbol{\omega}$, which in this case is perpendicular to the xy plane.

4.1. Free precession

The LLG equations for the Cartesian components of the magnetization are

$$\begin{aligned} \frac{\mathrm{d}}{\mathrm{d}t} M_x &= -\omega_\mathrm{L} M_z \sin(\omega t), \\ \frac{\mathrm{d}}{\mathrm{d}t} M_y &= \omega_\mathrm{L} M_z \cos(\omega t), \\ \frac{\mathrm{d}}{\mathrm{d}t} M_z &= \omega_\mathrm{L} (M_x \sin(\omega t) - M_y \cos(\omega t)). \end{aligned} \tag{16}$$

It is easy to find a special solution of these coupled equations for the case when $\mathrm{d}(M_z)/\mathrm{d}t = 0$, i.e. M_z is a time-independent constant:

$$\begin{aligned} M_x(t) &= \frac{\omega_\mathrm{L}}{\sqrt{\omega^2 + \omega_\mathrm{L}^2}} \cos(\omega t), \\ M_y(t) &= \frac{\omega_\mathrm{L}}{\sqrt{\omega^2 + \omega_\mathrm{L}^2}} \sin(\omega t), \\ M_z(t) &= \frac{\omega}{\sqrt{\omega^2 + \omega_\mathrm{L}^2}}. \end{aligned} \tag{17}$$

This solution is valid only for a special initial condition, namely, $M_x(0)/M_z(0) = \omega_\mathrm{L}/\omega$, $M_y(0) = 0$. For any other initial values, one has to find the general solution of equation (16). This can be done by means of an appropriate rotation into a coordinate system in which the LLG equations have the simplest possible solution: a time-independent magnetization vector. The transformation is done in three stages. The first rotation,

$$\underline{\underline{\mathrm{O}_1}} = \begin{pmatrix} +\cos(\omega t) & +\sin(\omega t) & 0 \\ -\sin(\omega t) & +\cos(\omega t) & 0 \\ 0 & 0 & 1 \end{pmatrix} \tag{18}$$

transforms the vector equation (16) into a coordinate system, which rotates around the z axis with the applied magnetic field. The transformed z axis points then in the direction of the angular velocity vector $\boldsymbol{\omega}$. The second rotation,

$$\underline{\underline{\mathrm{O}_2}} = \begin{pmatrix} +\cos(\Theta) & 0 & -\sin(\Theta) \\ 0 & 1 & 0 \\ +\sin(\Theta) & 0 & +\cos(\Theta) \end{pmatrix} \tag{19}$$

tilts the z axis into the direction of the angular velocity vector $\boldsymbol{\Omega} = \boldsymbol{\omega} + \boldsymbol{\omega}_\mathrm{L}$. As $\boldsymbol{\omega}_\mathrm{L}$ is aligned with **H**, it is perpendicular to $\boldsymbol{\omega}$, so that $|\boldsymbol{\Omega}| = \Omega = \sqrt{\omega^2 + \omega_\mathrm{L}^2}$ and $\cos(\Theta) = \omega/\Omega$ and $\sin(\Theta) = \omega_\mathrm{L}/\Omega$. Finally, the last rotation

$$\underline{\underline{\mathrm{O}_3}} = \begin{pmatrix} +\cos(\Omega t) & -\sin(\Omega t) & 0 \\ +\sin(\Omega t) & +\cos(\Omega t) & 0 \\ 0 & 0 & 1 \end{pmatrix} \tag{20}$$

is again a transformation into a rotating coordinate system. Similar rotations have been discussed in references [10] and [11]. In the new rotating coordinate system the transformed magnetization vector $(\underline{\underline{\mathrm{O}_3}} \cdot \underline{\underline{\mathrm{O}_2}} \cdot \underline{\underline{\mathrm{O}_1}}\mathbf{M}) = (M_\xi, M_\eta, M_\zeta)$ is found to be time independent. The inverse transformation $(\underline{\underline{\mathrm{O}_1^{-1}}} \cdot \underline{\underline{\mathrm{O}_2^{-1}}} \cdot \underline{\underline{\mathrm{O}_3^{-1}}})$ gives then the general solution of the LLG equation for circularly polarized applied field in the limit of vanishing Néel relaxation, which has the following form

$$\begin{aligned} M_x(t) = {} & \frac{\omega}{\Omega} \cos(\omega t)[M_\xi \cos(\Omega t) + M_\eta \sin(\Omega t)] \\ & + \sin(\omega t)[M_\xi \sin(\Omega t) - M_\eta \cos(\Omega t)] \\ & + \frac{\omega_\mathrm{L}}{\Omega} \cos(\omega t) \sqrt{1 - M_\xi^2 - M_\eta^2}, \\ M_y(t) = {} & \frac{\omega}{\Omega} \sin(\omega t)[M_\xi \cos(\Omega t) + M_\eta \sin(\Omega t)] \\ & - \cos(\omega t)[M_\xi \sin(\Omega t) - M_\eta \cos(\Omega t)] \end{aligned}$$

$$+\frac{\omega_{\rm L}}{\Omega}\sin(\omega t)\sqrt{1-M_\xi^2-M_\eta^2},$$

$$M_z(t) = -\frac{\omega_{\rm L}}{\Omega}[M_\xi\cos(\Omega t)+M_\eta\sin(\Omega t)] + \frac{\omega}{\Omega}\sqrt{1-M_\xi^2-M_\eta^2}, \tag{21}$$

where M_ξ and M_η are the Cartesian components of the magnetization vector in the rotated coordinate system. They are determined by the initial conditions as

$$M_\xi = \frac{\omega M_{x0}-\omega_{\rm L}\sqrt{1-(M_{x0})^2-(M_{y0})^2}}{\Omega}, \qquad M_\eta = M_{y0}. \tag{22}$$

(M_ξ and M_η are time independent). For non-vanishing relaxation, i.e. for $\alpha_{\rm N}\neq 0$, $M_\xi = M_\xi(t)$ and $M_\eta = M_\eta(t)$ become time dependent. It is easily verified that $M_\xi = M_\eta = 0$ implies the initial conditions for the validity of the special solution (17) and indeed equation (21) reduces to equation (17) in this case. In the limit of $\omega \to 0$, equation (21) recovers the solution (7) which is obtained for static applied field with $\alpha_{\rm N}\to 0$.

4.2. Damped precession

The LLG equations for the Cartesian components of the magnetization of a single magnetic nanoparticle in the presence of Néel relaxation, under circularly polarized applied field are

$$\begin{aligned}
\frac{\rm d}{{\rm d}t}M_x &= -\omega_{\rm L}M_z\sin(\omega t)+\alpha_{\rm N}[-M_xM_y\sin(\omega t) + (M_y^2+M_z^2)\cos(\omega t)],\\
\frac{\rm d}{{\rm d}t}M_y &= \omega_{\rm L}M_z\cos(\omega t)+\alpha_{\rm N}[-M_xM_y\cos(\omega t) + (M_x^2+M_z^2)\sin(\omega t)],\\
\frac{\rm d}{{\rm d}t}M_z &= \omega_{\rm L}[M_x\sin(\omega t)-M_y\cos(\omega t)] - \alpha_{\rm N}[M_xM_z\cos(\omega t)+M_yM_z\sin(\omega t)].
\end{aligned} \tag{23}$$

The general solution for arbitrary initial conditions can only be obtained numerically. It can be verified though that the LLG equations (23) are satisfied by the intuitively guessed solution

$$\begin{aligned}
M_x(t) &= M_{xy}\cos(\omega t-\varphi) = M_{x0}^{\rm spec}\cos(\omega t) - M_{y0}^{\rm spec}\sin(\omega t),\\
M_y(t) &= M_{xy}\sin(\omega t-\varphi) = M_{x0}^{\rm spec}\sin(\omega t) + M_{y0}^{\rm spec}\cos(\omega t),\\
M_z(t) &= \sqrt{1-(M_{x0}^{\rm spec})^2-(M_{y0}^{\rm spec})^2}
\end{aligned}, \tag{24}$$

where M_{xy} is the projection of the magnetization vector onto the xy plane, $M_{x0}^{\rm spec} = M_{xy}\cos(\varphi)$, $M_{y0}^{\rm spec} = -M_{xy}\sin(\varphi)$ and

$$\begin{aligned}
M_{x0}^{\rm spec} &= \sqrt{\frac{\alpha_{\rm N}^2-\omega_{\rm L}^2-\omega^2+\sqrt{4\alpha_{\rm N}^2\omega_{\rm L}^2+(\alpha_{\rm N}^2-\omega_{\rm L}^2-\omega^2)^2}}{2\alpha_{\rm N}^2}},\\
M_{y0}^{\rm spec} &= -\frac{\alpha_{\rm N}^2+\omega_{\rm L}^2+\omega^2-\sqrt{4\alpha_{\rm N}^2\omega_{\rm L}^2+(\alpha_{\rm N}^2-\omega_{\rm L}^2-\omega^2)^2}}{2\omega\alpha_{\rm N}}.
\end{aligned} \tag{25}$$

Equation (24) describes a precession around the z axis with a phase shift relative to the rotation of the magnetic field. However, there are conditions for the initial state: the phase shift is strictly determined by the tilt of the magnetization vector with respect to the z axis. The tilt is given by $\theta = \cos^{-1}(\sqrt{1-(M_{x0}^{\rm spec})^2-(M_{y0}^{\rm spec})^2})$, and the phase shift by $\varphi = \tan^{-1}(-M_{y0}^{\rm spec}/M_{x0}^{\rm spec})$. The relation between θ and φ is thus implicit in equation (25).

We have verified with countless numerical calculations that any other solution of the LLG equation (23) tends to equation (24) after a rather small transient time-interval. For the ensuing steady state the solutions of the LLG equation can be well approximated by equation (24). Similar asymptotic solution of the general LLG equation for rotating applied field has been discussed recently by Sun and Wang [10].

To understand the coupled dynamics of relaxation, precession and rotation, it is useful to rewrite the LLG equation with Néel relaxation, equation (23), and the special solution (24) in the rotating coordinate system defined in connection with the relaxation-free case. The transformed LLG equations read

$$\begin{aligned}
\frac{\rm d}{{\rm d}t}M_\xi &= \alpha_{\rm N}\left[-M_\xi M_\eta\frac{\omega}{\Omega}\sin(\Omega t) - M_\xi M_\zeta\frac{\omega_{\rm L}}{\Omega} + (1-M_\xi^2)\frac{\omega}{\Omega}\cos(\Omega t)\right]\\
\frac{\rm d}{{\rm d}t}M_\eta &= \alpha_{\rm N}\left[-M_\eta M_\xi\frac{\omega}{\Omega}\cos(\Omega t) - M_\eta M_\zeta\frac{\omega_{\rm L}}{\Omega} + (1-M_\eta^2)\frac{\omega}{\Omega}\sin(\Omega t)\right],\\
\frac{\rm d}{{\rm d}t}M_\zeta &= \alpha_{\rm N}\left[-M_\zeta M_\xi\frac{\omega}{\Omega}\cos(\Omega t) - M_\zeta M_\xi\frac{\omega}{\Omega}\sin(\Omega t) + (1-M_\zeta^2)\frac{\omega_{\rm L}}{\Omega}\right],
\end{aligned} \tag{26}$$

where (M_ξ, M_η, M_ζ) represents the magnetization vector in the rotated coordinate system. As $\mathbf{M}$ remains a unit vector in its transformed form, the LLG equations for the components M_ξ, M_η and M_ζ are not independent. The special solution (24) in terms of the rotating coordinates has the following form

$$\begin{aligned}
M_\xi(t) &= M_{\xi\eta}\cos(\Omega t-\varphi_a) = M_{\xi0}^{\rm spec}\cos(\Omega t) - M_{\eta0}^{\rm spec}\sin(\Omega t),\\
M_\eta(t) &= M_{\xi\eta}\sin(\Omega t-\varphi_a) = M_{\xi0}^{\rm spec}\sin(\Omega t) + M_{\eta0}^{\rm spec}\cos(\Omega t),\\
M_\zeta(t) &= \sqrt{1-(M_{\xi0}^{\rm spec})^2-(M_{\eta0}^{\rm spec})^2},
\end{aligned} \tag{27}$$

where $M_{\xi0}^{\rm spec} = M_{\xi\eta}\cos(\varphi_a)$, $M_{\eta0}^{\rm spec} = -M_{\xi\eta}\sin(\varphi_a)$ and similarly to equation (22), the time-independent parameters are

$$\begin{aligned}
M_{\xi0}^{\rm spec} &= \frac{\omega M_{x0}^{\rm spec}-\omega_{\rm L}\sqrt{1-(M_{x0}^{\rm spec})^2-(M_{y0}^{\rm spec})^2}}{\Omega},\\
M_{\eta0}^{\rm spec} &= M_{y0}^{\rm spec}.
\end{aligned} \tag{28}$$

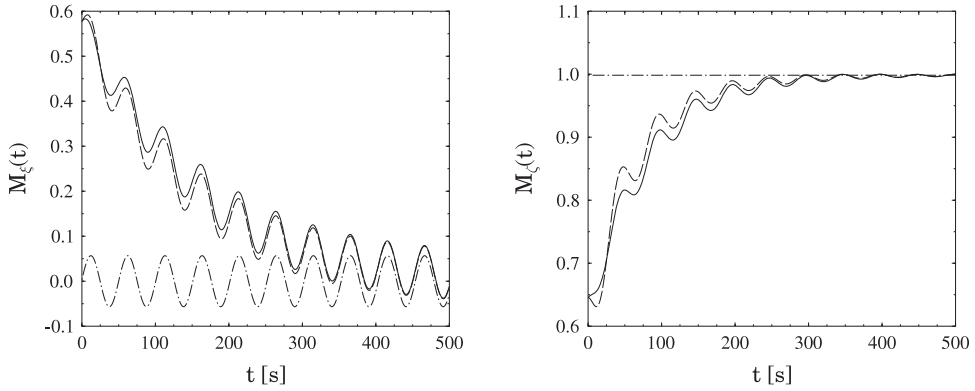

Figure 1. Numerical (full line), approximate (dashed line, see equation (29)) and the special (dashed-dotted line, see equation (27)) solutions of the LLG equations for the rotated coordinates $M_\xi(t)$ and $M_\zeta(t)$ of the magnetization are compared for $\omega = \omega_L = 0.088\ s^{-1}$, $\alpha = 0.14$.

The advantage of the rotating coordinate system is that the time dependence that stands for the rotation is embedded inside the relaxation term, showing that the motion is dominated by the trend towards the stationary solution by a characteristic time constant $\sim 1/\alpha_N$. Therefore, it represents a good framework to look for the general solution of the LLG equation or, alternatively, one can try to find approximate solutions of the LLG equation. For example

$$\begin{aligned} M_\xi(t) &= M_{\xi 0}^{\text{spec}} \cos(\Omega t) - M_{\eta 0}^{\text{spec}} \sin(\Omega t) \\ &\quad + (M_{\xi 0} - M_{\xi 0}^{\text{spec}}) e^{-\frac{\alpha_N t}{\sqrt{2}}}, \\ M_\eta(t) &= M_{\xi 0}^{\text{spec}} \sin(\Omega t) + M_{\eta 0}^{\text{spec}} \cos(\Omega t) \\ &\quad + (M_{\eta 0} - M_{\eta 0}^{\text{spec}})\, e^{-\frac{\alpha_N t}{\sqrt{2}}}, \\ M_\zeta(t) &= \sqrt{1 - [M_\xi(t)]^2 - [M_\eta(t)]^2}, \end{aligned} \tag{29}$$

well approximates the numerical solution of the LLG equation. The exponential decay of the last contributions to the in-plane components shows that the general solution converges quickly to the special solution. This is demonstrated in figure 1, for $\alpha_N = 0.01 s^{-1}$, ($\alpha = 0.14$) and $\omega = \omega_L = 0.088\ s^{-1}$, where the numerical and approximate solutions of the LLG equation are compared. The other consequence of the short transient process is that, irrespective of the initial conditions, the magnetization vector lies in the plane of the rotation, where it follows the driving field with a constant phase slip.

We note that both in the limits of weak and strong relaxation the phase slip φ goes to zero. This is seen in the values of the parameters in equation (25) of the special solution (24) in the appropriate limits:

$$M_{x0}^{\text{spec}}(\alpha_N \to 0) = \frac{\omega_L}{\sqrt{\omega^2 + \omega_L^2}}, \qquad M_{y0}^{\text{spec}}(\alpha_N \to 0) = 0, \tag{30}$$

and

$$M_{x0}^{\text{spec}}(\alpha_N \to 10^8 s^{-1}) \approx 1, \qquad M_{y0}^{\text{spec}}(\alpha_N \to 10^8 s^{-1}) \approx 0, \tag{31}$$

as in the limit of strong-relaxation $\alpha_N \approx 10^8\ s^{-1}$ values can be achieved. In general, the phase slip will depend on $\omega_L(H)$ and ω according to the relation $\varphi = \tan^{-1}(-M_{y0}^{\text{spec}}/M_{x0}^{\text{spec}})$.

4.3. Specific loss power

To calculate the energy loss per cycle for a single particle we use equation (11) again. The special solution (24) can be used to assess the merits of circular polarization, because in hyperthermia the field is applied for a long time ($\approx 10^3$ s) compared to the duration of the initial transient process ($\approx 10^{-6}$ s). Using this special solution, the dot product in equation (11) turns out to be integrable and the energy loss per cycle is found to be

$$E = \mu_0 2\pi m_S H(-M_{y0}^{\text{spec}}). \tag{32}$$

The weak-relaxation (or high-frequency) limit, $\alpha_N \ll \omega, \omega_L$, can be studied by means of a Taylor expansion of $(-M_{y0}^{\text{spec}})$, in powers of $\alpha_N^2/(\omega_L^2 + \omega^2)$. The result,

$$E \approx 2\pi \mu_0 m_S H \left[\frac{\omega^2}{\omega_L^2 + \omega^2} \left(\frac{\alpha_N}{\omega} \right) - \frac{\omega^4 \omega_L^2}{(\omega_L^2 + \omega^2)^3} \left(\frac{\alpha_N}{\omega} \right)^3 \right] \tag{33}$$

shows that there is no dissipation without relaxation. Making use of the relation $\alpha_N = \alpha\omega_L$ this expression can be written in a form that highlights the scaling of the variables:

$$E \approx 2\pi \mu_0 m_S H \frac{\omega}{\omega_L} \left[\left(\frac{\alpha}{1 + (\omega/\omega_L)^2} \right) - \left(\frac{\alpha}{1 + (\omega/\omega_L)^2} \right)^3 \right]. \tag{34}$$

The loss per cycle for strong relaxation (or low frequency), $\alpha_N \gg \omega, \omega_L$, shows similar scaling relations

$$E \approx 2\pi \mu_0 m_S H \left[\frac{\alpha_N^2}{\omega_L^2 + \alpha_N^2} \left(\frac{\omega}{\alpha_N} \right) - \frac{\alpha_N^4 \omega_L^2}{(\omega_L^2 + \alpha_N^2)^3} \left(\frac{\omega}{\alpha_N} \right)^3 \right], \tag{35}$$

and

$$E \approx 2\pi \mu_0 m_S H \frac{\omega}{\omega_L} \left[\left(\frac{\alpha}{1 + (\alpha)^2} \right) - \left(\frac{\alpha}{1 + (\alpha)^2} \right)^3 \right]. \tag{36}$$

We emphasize that the distinction between ω_L and the 'bare' Larmor frequency $\omega_{L0} = \mu_0 \gamma_0 H$ cannot be ignored in the strong-relaxation limit. In fact, the definition $\alpha_N = \omega_{L0}\alpha/(1 + \alpha^2)$ makes the limit $\alpha_N \to \infty$ meaningless, because the largest value of α_N is $\omega_{L0}/2$, which is realized at $\alpha = 1$.

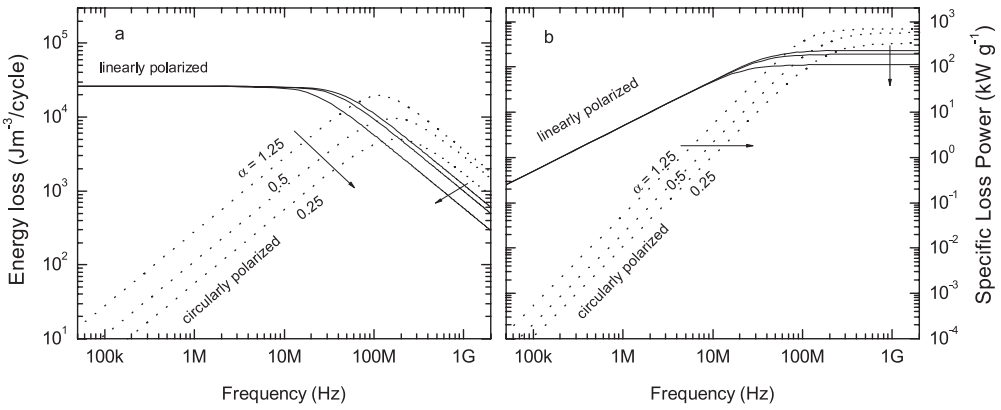

Figure 2. Energy loss per cycle (a) and specific loss power (b) for linearly and circularly polarized fields for magnetite as a function of driving field frequency for different α damping parameters. Arrows point towards the direction of decreasing α. Driving field amplitude $H = 10^4$ A m^{-1}.

5. Conclusion and summary

We have reported numerical and analytical results on the response of an immobilized single-domain magnetic particle under linearly and circularly polarized magnetic fields. Comparison of the dynamics in the presence and absence of Néel relaxation enables an interpretation of the results in terms of an interplay between Larmor precession and relaxation towards energy minima.

In figure 2(a) the resulting energy loss per cycle is depicted as a function of frequency and the dimensionless damping parameter α. Regarding the merits of linear or circular polarization of the magnetic field, we find opposite preferences for frequencies below and above the Larmor frequency. In the former case, which is relevant to hyperthermia, the energy absorbed by the magnet from linearly polarized field exceeds the absorption from rotating field by orders of magnitude. Apparently the relaxation towards a steady state with a small phase shift between the rotating **H** and **m** fields ensures a smooth process with very small losses. This cannot take place in a linear field, where the orientation of **H** changes abruptly twice in a cycle and relaxation towards the new energy minimum has to be repeated. In the case of high frequencies, which is not lacking technological relevance since the recent interest in materials with high microwave absorption [12], the relaxation is slow compared to the rate of change of the magnetic field and the loss per cycle becomes frequency dependent.

The tent-shaped curves in figure 2(a) reflect the relevance of the limiting cases worked out in sections 3.3 and 4.3. The low-frequency behaviour, which seems to prevail through many orders of magnitude in frequency, reflects equation (10) for the case of linear polarization and the first term in equation (34) for rotating field. Equation (10) describes a relaxation process, which takes place after each change of sign of H_x, apparently at the same cost in energy as long as the period of the oscillation of the field is much larger than the relaxation time. The loss per cycle is then always the same and we see no dependence on the damping constant either, except that for weaker damping the deviation from the constant value begins at a lower frequency. Equation (34) shows clearly that for frequencies much lower than the Larmor frequency the loss is always proportional to the frequency, the slope scaling with the dimensionless damping factor α (in the log–log plot this translates to straight lines with the same slope, shifted by distances scaling with α). In contrast, equations (13) and (33) show that, in both cases, at high frequencies the loss is proportional to α_N/ω, which explains why all curves run parallel, with the same slope, and the dependence of their position on α is not monotonic.

Figure 2(b) shows the same data in practical units, that is, it shows the proper specific absorption power in W g^{-1} for a single-domain particle of magnetite. At frequencies relevant to hyperthermia ($\sim 10^5$ Hz) with linearly polarized field, respectable losses of kW g^{-1} order can be achieved, while the power absorbed from circularly polarized field is two to three orders of magnitude lower. Our final conclusion is obvious: if Néel relaxation in isotropic sample is the dominant mechanism, the technical complications of generating a circularly polarized field in difficult geometry need not be considered.

Acknowledgment

The authors acknowledge support from the Hungarian National Office for Research and Technology NKFP-5/006/2005, Contract OM-00077/2005.

References

[1] Einstein A and de Haas W J 1915 *Proc. R. Dutch Acad. Sci.* **17** 152–70
Einstein A and de Haas W J 1915 *Proc. R. Dutch Acad. Sci.* **17** 203–420
[2] Hergt R, Dutz S, Muller R and Zeisberger M 2006 *J. Phys.: Condens. Matter* **18** S2919
Hergt R and Dutz S 2007 *J. Magn. Magn. Mater.* **311** 187
[3] Coffey W T and Fannin P C 2002 *J. Phys.: Condens. Matter* **14** 3677
Moroz P, Jones S K and Gray B N 2002 *Int. J. Hyperth.* **18** 267
[4] Landau L D and Lifshitz E M 1935 *Phys. Z. Sowj.* **8** 153

[5] Néel L 1949 *C. R. Acad. Sci. (Paris)* **228** 664
[6] Gilbert T L 1956 *Phys. Rev.* **100** 1243
[7] Brown W F Jr 1979 *IEEE Trans. Magn.* **15** 1196
[8] Kikuchi R 1956 *J. Appl. Phys.* **27** 1352
[9] Mallinson J C 1987 *IEEE Trans. Magn.* **23** 2003
[10] Sun Z Z and Wang X R 2006 *Phys. Rev.* B **73** 092416
[11] Denisov S I, Lyutyy T V, Hänggi P and Trohidou K N 2006 *Phys. Rev.* B **74** 104406
[12] Li X G, Geng D Y, Meng H, Shang P J and Zhang Z D 2008 *Appl. Phys. Lett.* **92** 173117